J|A|C|S
ARTICLES
Published on Web 03/09/2006

Molecular Wiring of Nanocrystals: NCS-Enhanced Cross-Surface Charge Transfer in Self-Assembled Ru-Complex Monolayer on Mesoscopic Oxide Films

Qing Wang, Shaik M. Zakeeruddin, Md. K. Nazeeruddin, Robin Humphry-Baker, and Michael Grätzel*

Contribution from the Laboratory for Photonics and Interfaces, Ecole Polytechnique Fédérale, CH-1015 Lausanne, Switzerland

Received December 20, 2005; E-mail: michael.graetzel@epfl.ch

Abstract: We report on rapid ambipolar cross-surface charge transfer within self-assembled monolayers (SAM) of the heteroleptic Ru-complexes *cis*-RuLL′(NCS)$_2$ (L = 2,2′-bipyridyl-4,4′-dicarboxylic acid, L′ = 4,4′-dinonyl-2,2′-bipyridyl) (**1**) and *cis*-RuLL″(NCS)$_2$ (L = 2,2′-bipyridyl-4,4′-dicarboxylic acid, L′ = 4,4′-dimethyl-2,2′-bipyridyl) (**2**) on the surface of mesoscopic insulating oxide films. The bipyridyl ligands of the Ru-complex transport electrons, while the NCS groups plays a pivotal role in mediating surface confined hole percolation. Molecular dynamics calculations show the NCS ligands of **1** and **2** to orient in a fashion that enhances the overlap of the HOMOs of neighboring ruthenium complexes. Using ab initio Hartree−Fock calculations the electronic coupling matrix element for intermolecular hole exchange at the surface is estimated to be 0.13 eV. Cyclic voltammetry as well as spectroelectrochemical and impedance measurements performed with a series of other Ru-complexes confirmed the control of the cross surface charge transfer by the molecular structure. Complex **2** shows the highest percolation rate, the surface hole diffusion coefficient being 1.1 × 10^{-8} cm^2/s. The effects of the ligand properties, such as denticity, geometry, and size, on the intermolecular charge transport are discussed in detail.

Introduction

While charge transfer reactions, both on the molecular and on the bulk level, are presently fairly well understood,[1] their characterization on the mesoscopic scale is only at its beginning.[2] These nanoscale electron transfer processes, however, are important to both the frontier of fundamental science and applications to organic-based electronic materials, including areas such as miniaturized transistors, sensors, electroluminescent and electrochromic displays, electrocatalysis, biofuel cells, and solar photoconversion.[3] Exploring lateral charge transport in self-assembled monolayers (SAMs) of redox active molecules is of particular interest in this context. As indicated schematically in Figure 1, a monolayer of redox active molecules is adsorbed on the surface of a nanocrystalline oxide film, which is deposited on a conducting glass (fluorine doped tin oxide, FTO). Upon applying a positive polarization to the electrode, holes are injected into the film via the molecules attached to the FTO and propagate along the surface. At the same time, counterions in electrolyte diffuse to counter balance the charge of the oxidized molecules. Consequently, the whole molecular monolayer becomes electrochemically addressable by the lateral charge percolation. The equivalent circuit shown in Figure 1 depicts the hole percolation channel and electrolyte diffusion channel two transmission lines which are coupled by a capacitive

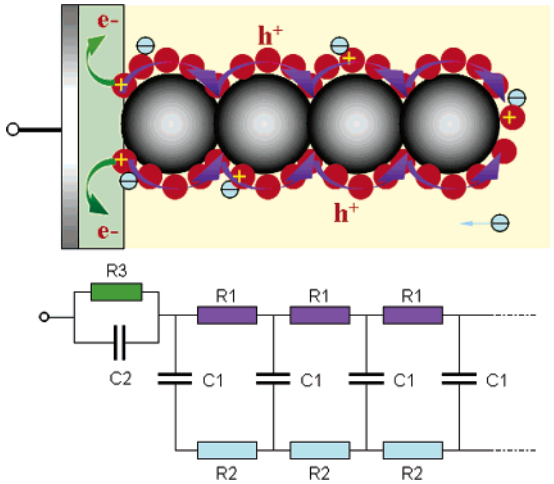

Figure 1. Schematic model showing the cross surface charge percolation through the molecular monolayer adsorbed on mesoscopic oxide films. Equivalent circuit showing the charge percolation channel through the molecular monolayer (R1) and diffusion channel of counterion in the electrolyte (R2). C1 is the chemical capacitance of the molecular monolayer. R3 is the charge transfer impedance of the molecule at the FTO/electrolyte interface. C2 is the corresponding double layer capacitance.

(1) Jortner, J.; Bixon, M. *Adv. Chem. Phys.* **1999**, *106*, 1−734.
(2) Datta, S. *Electronic transport in mesocopic systems*; Cambridge University Press: Cambridge, UK: 1995.
(3) (a) Bonhôte, P.; Gogniat, E.; Campus, F.; Walder, L.; Grätzel, M. *Displays* **1999**, *20*, 137−144. (b) Cummins, D.; Boschloo, G.; Ryan, M.; Corr, D.; Rao, S. N.; Fitzmaurice, D. *J. Phys. Chem. B* **2000**, *104*, 11449−11459. (c) Gopel, W.; Schierbaum, K. D. *Sensors and Actuators, B: Chemical* **1995**, *26*, 1−12. (d) Long, B.; Nikitin, K.; Fitzmaurice, D. *J. Am. Chem. Soc.* **2003**, *125*, 5152−5160. (e) Heller, A. *Phys. Chem. Chem. Phys.* **2004**, *6*, 209−216. (f) O'Regan, B.; Gräzel, M. *Nature* **1991**, *353*, 737−740. (g) Grätzel, M. *Nature* **2001**, *414*, 338−344.

10.1021/ja058616h CCC: $33.50

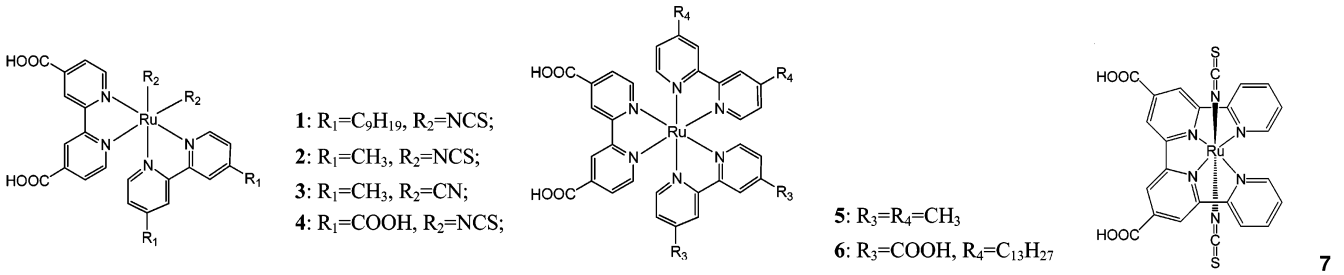

Figure 2. Ru-complexes used in this study.

element to account for the charge balance process at the molecule/electrolyte interface. An analogous electric circuit diagram can be drawn for electron percolation.

Charge propagation within the surface confined monolayer proceeds by thermally activated electron hopping between adjacent dye molecules. A macroscopic conduction pathway is formed once the coverage of the oxide nanoparticles by the electroactive species exceeds 50%.[4] Good spatial overlap of the adjacent molecular orbitals (MOs) and a low reorganization energy are required to achieve high percolation rates.[5] Previous studies were mainly focused on organic molecules, such as triarylamine, perylene derivatives, etc.[4] Transition metal complexes are attractive candidates to function as surface-anchored electron relays, due to their chemical stability as well as their tunable optical and redox properties.[6] However, so far very few studies have been performed in this area.[7] Meyer et al. have studied the lateral charge hopping within an $[Os^{II}(bpy)_2(4,4'\text{-dcbpy})](PF_6)_2$ monolayer assembled on a mesoscopic TiO_2 film, yielding a hole diffusion coefficient of 1.4×10^{-9} cm^2/s.[7a] To our knowledge, electron conduction by the polypyridine ligands of the transition metal has not been reported so far.

Ruthenium polypyridyl complexes attached onto mesoscopic oxide films are of particular interest as they remain to date the most efficient sensitizers for dye-sensitized solar cells (DSC).[3f,3g] Understanding the electronic interaction between the dye molecules is essential for the rational design and realization of devices with improved performance. Here we report on rapid ambipolar cross-surface charge transfer within self-assembled monolayers (SAM) of a series of such Ru-complexes. We demonstrate for the first time the ability of the bpy-ligands to conduct electrons along the surface and reveal the pivotal role played by the NCS-ligands in greatly enhancing the hole transport within the SAM. The effect of electronic coupling and nuclear reorganization on the dynamics of this intriguing process is also scrutinized.

Experimental Section

Materials. The structures of ruthenium complexes used in this study are displayed in Figure 2. Their synthesis has been described elsewhere.[8] *n*-Hexadecylmalonic acid (HDMA) and tetra-*n*-butylammonium hexafluorophosphate ($TBAPF_6$) were purchased from Lancaster and Fluka, respectively. 1-Ethyl-3-methylimidazolium bis(trifluoromethanesulfonyl)amide (EMITFSI) was synthesized according to literature procedure.[9]

Preparation of Mesoscopic Oxide Film. The TiO_2 colloid was prepared using a published procedures.[10] A paste consisting of 20 nm TiO_2 colloid and ethyl cellulose in terpineol was deposited using the doctor blade technique on a fluorine-doped SnO_2 conducting glass (TEC15, 15Ω/cm) to form a transparent layer. Subsequently, the deposited film was heated to 500 °C in an oxygen atmosphere and calcined for 10 min. The final film thickness was determined by using an Alpha-step 200 surface profilometer (Tencor Instruments, USA) to be ca. 5.5 μm. A porosity of 0.63 and roughness factor of ~110 per micron for the transparent layer were measured with a Gemini 2327 nitrogen adsorption apparatus (Micromeretics Instrument Corp., USA). The mesoscopic Al_2O_3 film with a particle size of 6 nm was prepared as described in ref 4a. The mesoscopic metal oxide films were first sintered at 500 °C for 20 min in air and after cooling to 80 °C immersed overnight in a solution of 0.30 mM Ru-complex in a mixture of acetonitrile and *tert*-butyl alcohol (volume ratio, 1:1). The surface coverage was determined by UV/vis measurements. Mixed layers containing the redox-inactive HDMA were analyzed by UV−visible absorption spectroscopy, and their content of adsorbed ruthenium complex was derived from the absorbance change of the film at 530 nm. It was assumed that solution containing the ruthenium complex alone gives full monolayer coverage.

UV−vis and ATR-FTIR Measurements. UV−vis spectra were measured on a Cary 5 spectrophotometer. ATR-FTIR analysis employed a FTS700 FTIR spectrometer (Digilab, USA). Samples were measured under a mechanical force pushing the surface in contact with the diamond window. Spectra were derived from 64 scans at a resolution of 4 cm^{-1}. Prior to measuring the spectra, the dyed films were rinsed in acetonitrile to wash out any weakly adsorbed molecules and dried. Spectroelectrochemical measurements were carried out with a three-electrode optic cell on a Cary 5 spectrophotometer. The electrolyte was 0.1 M $TBAPF_6$ dissolved in acetonitrile. The electrode potential was controlled by a PC-controlled AutoLab PSTAT10 electrochemical workstation (Eco Chimie). The UV−vis spectra were collected by polarizing the electrode at different potentials until the current drops to $^1/_{10}$ of the initial value.

Electrochemical Measurements. Voltammetric measurements employed a PC-controlled AutoLab PSTAT10 electrochemical workstation.

(4) (a) Bonhôte, P.; Gogniat, E.; Tingry, S.; Barbé, C.; Vlachopoulos, N.; Lenzmann, F.; Comte, P.; Grätzel, M. *J. Phys. Chem. B* **1998**, *102*, 1498−1507. (b) Westermark, K.; Tingry, S.; Persson, P.; Rensmo, H.; Lunell, S.; Hagfeldt, A.; Siegbahn, H. *J. Phys. Chem. B* **2001**, *105*, 7182−7187. (c) Wang, Q.; Zakeeruddin, S. M.; Cremer, J.; Bäuerle, P.; Humphry-Baker, R.; Grätzel, M. *J. Am. Chem. Soc.* **2005**, *127*, 5706−5713.
(5) Lin, B. C.; Cheng, C. P.; You, Z.; Hsu, C. *J. Am. Chem. Soc.* **2005**, *127*, 66−67.
(6) For example, see: Juris, A.; Balzani, V. *Coord. Chem. Rev.* **1988**, *84*, 85−277.
(7) (a) Trammell, S. A.; Meyer T. J. *J. Phys. Chem. B* **1999**, *103*, 104−107. (b) Aranyos, V.; Grennberg, H.; Tingry, S.; Lindquist, S.-E.; Hagfeldt, A. *Solar Energy Materials & Solar Cells* **2000**, *64*, 97−114. (c) Andersson, A. M.; Isovitsch, R.; Miranda, D.; Wadhwa, S.; Schmehl, R. H. *Chem. Commun.* **2000**, 505−506. (d) Galoppini, E.; Guo, W. Z.; Zhang, W., Hoertz, P. G.; Qu, P.; Meyer, G. J. *J. Am. Chem. Soc.* **2002**, *124*, 7801−7811. (e) Aranyos, V.; Hjelm, J.; Hagfeldt, A.; Grennberg, H. *Dalton Trans.* **2003**, 1280−1283.
(8) (a) Nazeeruddin, M. K.; Kay, A.; Rodicio, I.; Humphry-Baker, R.; Muller, E.; Liska, P.; Vlachopoulos, N.; Grätzel, M. *J. Am. Chem. Soc.* **1993**, *115*, 6382−6390. (b) Zakeeruddin, S. M.; Nazeeruddin, M. K.; Humphry-Baker, R.; Péchy, P.; Quagliotto, P.; Barolo, C.; Viscardi, G.; Grätzel, M. *Langmuir* **2002**, *18*, 952−954.
(9) Bonhôte, P.; Dias, A. P.; Papageorgiou, N.; Kalyanasundaram, K.; Grätzel, M. *Inorg. Chem.* **1996**, *35*, 1168−1178.
(10) Barbe, C. J.; Arendse, F.; Comte, P.; Jirousek, M.; Lenzmann, F.; Shklover, V.; Grätzel, M. *J. Am. Ceram. Soc.* **1997**, *80*, 3157−3171.

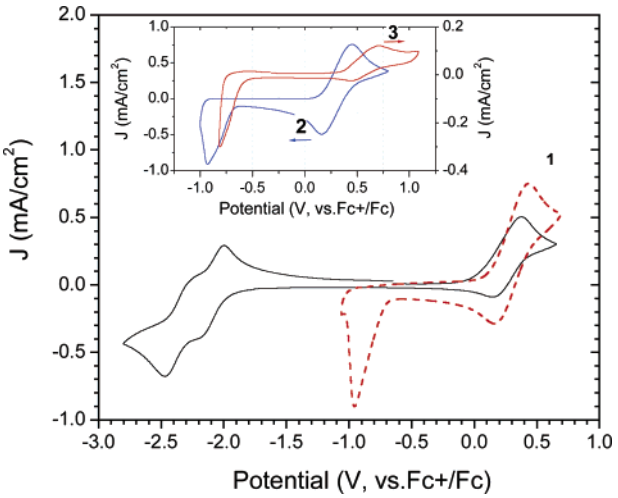

Figure 3. Cyclic voltamogram of complex **1** adsorbed on mesoscopic TiO_2 (dash red) and Al_2O_3 (solid black) films. The electrolyte is 0.1 M EMITFSI/acetonitrile. The scan rate is 0.1 V/s. The inset shows the CV of complex **2** (blue) and **3** (red) adsorbed on TiO_2. The right ordinate scale applies to the red curve. The electrolyte is pure EMITFSI. The scan rate is 0.1 V/s for all curves.

Cyclic voltammograms (CV) were obtained at different scan rates using 0.1 M EMITFSI in acetonitrile and pure EMITFSI as the electrolyte, and the mesoscopic metal oxide film as working electrode. Chronocoulometric measurements were carried out under the same conditions. Impedance analysis was performed with a computer-controlled potentiostat (EG&G, M273) equipped with a frequency response analyzer (EG&G, M1025). The frequency range is 0.01 Hz−100 kHz. The magnitude of the alternative signal is 5 mV. The electrolyte is 0.1 M $TBAPF_6$ in acetonitrile. In all cases a platinum coil and Ag/AgCl electrode were employed as the counter and reference electrode, respectively. Unless otherwise mentioned, the potentials reported below use the ferrocene/ferrocinium (Fc^+/Fc) couple as an internal reference.

Results

The heteroleptic amphiphilic ruthenium complex *cis*-RuLL′(NCS)$_2$ (L = 2,2′-bipyridyl-4,4′-dicarboxylic acid, L′ = 4,4′-dinonyl-2,2′-bipyridyl) (**1**) has gained prominence as the first sensitizer sustaining stable DSC operation under long-term light soaking and high-temperature stress.[11] Figure 3 shows the CV of **1** adsorbed on mesoscopic TiO_2 and Al_2O_3 films. Strikingly, despite the insulating nature of the mesoscopic electrodes a chemically reversible anodic wave appears at ∼0.40 V (vs Fc+/Fc) on both films indicating the occurrence of one-electron oxidation of Ru^{II} to Ru^{III}. For the Al_2O_3 film two additional $1e^-$ reduction waves appear at −1.80 and −2.15 V (vs Fc+/Fc) that are attributed to the stepwise reduction of the bipyridine ligands under formation of radical anions. Similar redox waves are observed with acetonitrile solutions of this complex.

Figure 4a shows spectroelectrochemical measurements carried out with complex **1** adsorbed on the mesoscopic TiO_2 film. As the applied potential is scanned from −0.4 to 0.5 V (vs Fc+/Fc), a new broad feature appears at around 770 nm in the UV/vis spectrum arising from the ligand-to-metal charge transition (LMCT) of the Ru(III) complex.[12] Concomitantly the characteristic metal to ligand charge transfer (MLCT) absorption bands

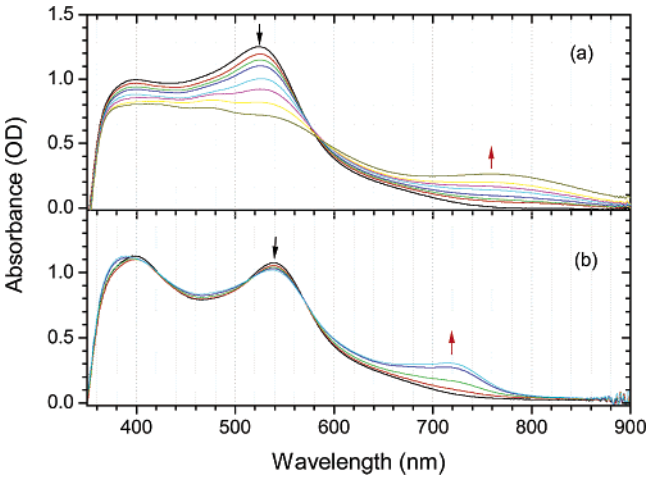

Figure 4. UV/vis spectra of complex **1** (a) and **4** (b) adsorbed mesoscopic TiO_2 electrodes measured at different potentials. The potential range is from −0.4 to 0.5 V (vs Fc+/Fc). The voltage increment for each spectroscopic scan is 50 mV. The electrolyte is 0.1 M $TBAPF_6$/acetonitrile.

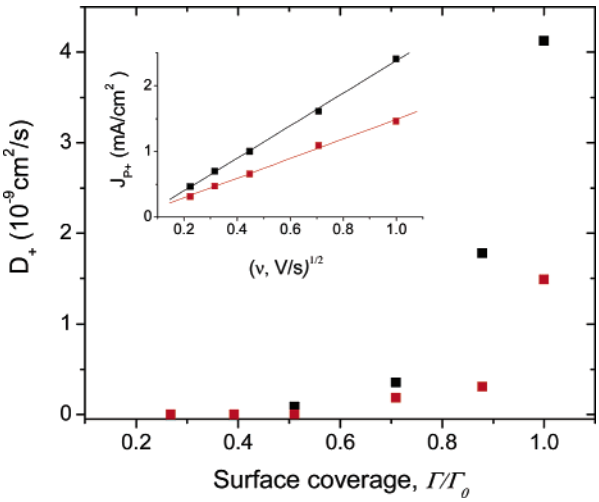

Figure 5. D_+ of charge percolation in monolayer of complex **1** adsorbed on mesoscopic TiO_2 as a function of Γ/Γ_0. HDMA was used as diluent. The electrolytes are 0.1 M EMITFSI/acetonitrile (black) and pure EMITFSI (red). The inset shows the forward peak current as a function of the square root of scan rate, $\nu^{1/2}$.

of the Ru(II) complex at 400 nm and 525 nm are bleached. The appearance of a clean isosbestic point at 580 nm confirms that a simple one-step conversion of the Ru(II) to the Ru(III) takes place when the polarization of the FTO electrode reaches the redox potential of the surface adsorbed sensitizer. The lifetime of the oxidized sensitizer is about 75 min on the mesoscopic TiO_2 film,[13] which is much longer than the measurement time in Figure 3. Because the substrate films are insulating in the examined potential range and **1** is tightly bound to the oxide surface, a cross surface charge propagation mechanism is suggested and is confirmed by the appearance of a percolation threshold.

As shown in the inset of Figure 5, the peak current of the anodic wave in the CV is proportional to the square root of the scan rate ($\nu^{1/2}$), indicating a semi-infinite diffusion controlled charge transport process, the thickness of the depletion layer

(11) Wang, P.; Zakeeruddin, S. M.; Moser, J. E.; Nazeeruddin, M. K.; Sekiguchi, T.; Grätzel, M. *Nat. Mater.* **2003**, *2*, 402−407.
(12) (a) Tachibana, Y.; Moser, J. E.; Grätzel, M.; Klug, D. R.; Durrant, J. R. *J. Phys. Chem.* **1996**, *100*, 20056−20062. (b) Moser, J. E.; Noukakis, D.; Bach, U.; Tachibana, Y.; Klug, D. R.; Durrant, J. R.; Humphry-Baker, R.; Grätzel, M. *J. Phys. Chem. B* **1998**, *102*, 3649−3650.
(13) Wang, P.; Wenger, B.; Humphry-Baker, R.; Moser, J.-E.; Teuscher, J.; Kantlehner, W.; Mezger, J.; Stoyanov, E. V.; Zakeeruddin, S. M.; Grätzel, M. *J. Am. Chem. Soc.* **2005**, *127*, 6850−6856.

being smaller than the film thickness. For a reversible system, the diffusion coefficients (D_+) describing the cross surface motion of holes through the SAM of complex **1** can be derived from the slope of the straight line using the equation[14]

$$i_p = (2.69 \times 10^5) n^{3/2} A D_+^{1/2} c_o \nu^{1/2} \quad (1)$$

where n is the number of electrons involved in the exchange reaction, A is the electrode area, and c_o is the concentration of the sensitizer in the film. Assuming complete monolayer coverage, a TiO_2 particle size of 20 nm, and a porosity of 60%, c_o is derived to be ca. 138 mM, and D_+ is calculated to be 4.1×10^{-9} and 1.5×10^{-9} cm^2/s in the 0.1 M EMITFSI/acetonitrile solution and pure EMITFSI, respectively.[15] Using HDMA as spacer molecule, D_+ was determined at various surface coverages. Charge hopping is only observed above a threshold concentration where the complex occupies ca. 50% of the TiO_2 surface, in agreement with theoretical predictions for two-dimensional charge percolation.[16] The presence of a percolation threshold excludes that translational motion of the ruthenium complex along the TiO_2 surface makes a significant contribution to the observed current.[4a,4c] In addition, the percolation rate in the acetonitrile-based electrolyte is faster than that in the pure ionic liquid. This solvent dependence is attributed to the slower diffusion[17] of charge compensating anions in the ionic liquid, whose viscosity is about 100 times larger than that of the acetonitrile-based electrolyte.[18]

Discussion

The rate of intermolecular electron exchange can be described by the Marcus theory given in eq 2,[19]

$$k_{et} = \frac{2\pi}{\hbar} \frac{H_{da}^2}{\sqrt{4\pi\lambda kT}} \exp\left[-\frac{(\lambda + \Delta G^\circ)^2}{4\lambda kT}\right] \quad (2)$$

where λ is the reorganization energy, H_{da} is the electronic coupling between the donor and acceptor sites, and ΔG° is the standard free energy for the electron transfer. It is clear that good electronic coupling and a low reorganization energy are required for the charge transport in the surface-confined molecular layer to occur rapidly.

Raman spectroscopic studies have shown that total reorganization energy (vibrational and solvent) of complex **4** is the lowest reported so far, i.e., 152 meV in DMSO and only 34 meV when adsorbed on the surface of mesoscopic TiO_2.[20] The 5-fold decrease of λ was attributed to the increased rigidity of the molecule in the adsorbed state and to a restriction of solvation due to the fact that the TiO_2 particles block the access of the solvent to the complex. The Raman spectra of the heteroleptic complex **1** and **2** on the TiO_2 surface are very similar to that reported for complex **4**. This would suggest that the reorganization energy is also low rendering the charge hopping between neighboring molecules of **1** or **2** practically barrierless. Therefore, electronic coupling is likely to be the dominant term that controls the rate of cross-surface hole percolation along with charge compensating diffusion of anions in the pores.

The specific fashion in which complexes **1** and **2** are anchored to the oxide is presumably responsible for the strong intermolecular electronic coupling and the observed facile cross-surface charge transport. The IR spectra of **2** in Figure 6 confirm coordinative binding of the two carboxylate groups to surface titanium ions.[21] The presence of the 4,4′-dialkyl-2,2′-bipyridyl ligand imposes a configuration in the adsorbed state where the sulfur atoms of adjacent dye molecules are estimated to be only 0.4 nm apart (the distance between Ru-centers of neighboring complexes being 1.1 nm). The large spatial expansion of the sulfur *p*-orbitals forming an important part of the HOMO of complex **1** and **2**[22] results in significant MO overlap favoring rapid lateral hole exchange. Molecular orbital calculations performed on complex **2** confirm that the electronic interaction between neighboring molecules is indeed very sensitive to their configuration on the TiO_2 surface. For the optimal spatial arrangement of **2** on an anatase (101) surface, the coupling term is derived to be 0.13 eV using an ab initio Hartree−Fock calculation as described in ref 5.

The crucial role played by the NCS ligand in promoting cross-surface hole transport is substantiated by electrochemical experiments employing the ruthenium complex $RuLL''(CN)_2$ (L″ = 4,4′-dimethyl-2,2′-bipyridyl) (**3**), which has a similar structure to **1** and **2** except that the thiocyanate ligands are replaced by cyanide. Figure 6b allows comparison of the FTIR spectrum of complex **3** with that of the monolayer adsorbed on a mesoscopic TiO_2 film. The IR spectra of complex **3** are similar in the pure and adsorbed state. Vibration from −CN stretching at 2080 cm^{-1} is clearly seen in the spectra for both samples. The band at 1720 cm^{-1} assigned to the C═O stretching of the carboxylic acid almost disappears upon adsorption on mesoscopic TiO_2. Meanwhile, new bands at 1387 and 1590 cm^{-1} assigned to the carboxylate symmetric and asymmetric $-CO_2$ stretching appear, indicating a strong interaction between the carboxylate group of the adsorbed molecules and the substrate. With respect to the adsorption of complex **2** as its spectrum illustrated in Figure 6a, the adsorption of **3** on the mesoscopic TiO_2 surface proceeds in a very similar fashion.

(14) Bard, A. J.; Faulkner, L. R. *Electrochemical Methods: Fundamentals and Applications*, 2nd ed.; John Wiley & Sons: 2000.
(15) It is a frequent observation that the diffusion coefficient measured by chronocoulometry is larger than that observed using cyclic voltammetry. This difference may reflect the variation in the density of redox centers through the film thickness causing an increased intersite separation and lower rates of charge transport. The redox composition of a significantly larger fraction of the layer is switched in the slower cyclic voltammetry experiments than in chronocoulometry. Intercalation of charge compensating counterions in the SAM may occur under these conditions impairing the charge transport. The diffusion coefficients derived from impedance measurements are assumed to be higher for a similar reason. See: Hogan, C. F.; Forster, R. J. *Analytica Chimica Acta* **1999**, *396*, 13−21.
(16) Sahimi, M. *Application of Percolation Theory*; Taylor & Francis: 1994; pp 1−22.
(17) For example, see: (a) Weaver, M. J. *Chem. Rev.* **1992**, *92*, 463−480. (b) Zhang, X.; Leddy, J.; Bard, A. J. *J. Am. Chem. Soc.* **1985**, *107*, 3719−3721.
(18) The observed diffusion coefficient D_+ is ambipolar, i.e., $(p + c)/D_+ = c/D_{h+} + p/D_{counterion}$, where D_{h+} is the charge diffusion rate in the complex monolayer, $D_{counterion}$ is the diffusion rate of counterions in the electrolyte, and p and c are the density of charges in the complex layer and counterions in the electrolyte, respectively. See: Kopidakis, N.; Schiff, E. A.; Park, N.-G.; van de Lagemaat, J.; Frank, A. J. *J. Phys. Chem. B* **2000**, *104*, 3930−3936.
(19) (a) Marcus, R. A.; Sutin, N. *Biochim. Biophys. Acta* **1985**, *811*, 265−322. (b) Adams, D. M. et al. *J. Phys. Chem. B* **2003**, *107*, 6668−6697.
(20) Shoute, L. C. T.; Loppnow, G. R. *J. Am. Chem. Soc.* **2003**, *125*, 15636−15646.
(21) Nazeeruddin, M. K.; Humphry-Baker R.; Liska, P.; Grätzel, M. *J. Phys. Chem. B* **2003**, *107*, 8981−8987.
(22) (a) Rensmo, H.; Södergren, S.; Patthey, L.; Westermark, K.; Vayssieres, L.; Kohle, O.; Brühwiler, P. A.; Hagfeldt, A.; Siegbahn, H. *Chem. Phys. Lett.* **1997**, *274*, 51−57. (b) Rensmo, H.; Lunell, S.; Siegbahn, H. *J. Photochem. Photobiol. A* **1998**, *114*, 117−124.

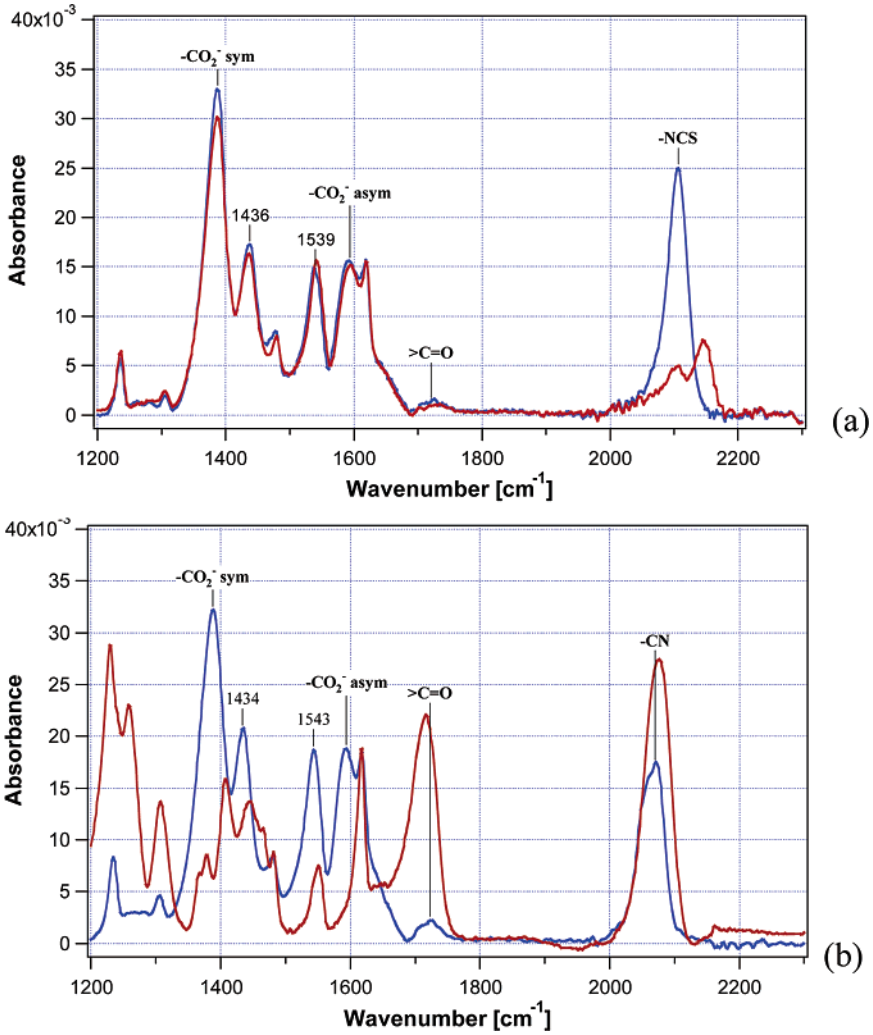

Figure 6. Normalized ATR-FTIR spectra of (a) mesoscopic TiO_2 film with saturated surface concentration of complex **2** before (blue line) and after dipping in 25 mM $HgCl_2$/acetonitrile solution (red line); (b) complex **3** powder (red line) and mesoscopic TiO_2 film with saturated surface concentration of complex **3** (blue line).

The HOMO of **3**, due to the absence of sulfur atoms, is contracted resulting in greatly reduced MO-overlap between adjacent dye molecules, as seen in Figure 7. As a consequence, a monolayer of complex **3** immobilized on the surface of the mesoscopic TiO_2 film is unable to transport holes efficiently. This is apparent from the inset of Figure 3 where the height of the anodic peak current observed with complex **3** is almost seven times smaller than that of **2**, EMITFSI being used as the electrolyte. In addition, no appreciable difference in the redox potential of **3** was observed when it was adsorbed on TiO_2 or FTO substrate, excluding the possibility that the FTO adsorbed complex could trap holes impairing their transfer to adjacent complex molecules adsorbed on the mesoscopic TiO_2 film.

Slow charge percolation through the SAM of complex **3** is also corroborated by impedance measurements using 0.1M $TBAPF_6$/acetonitrile as the electrolyte. As shown in Figure 8, both complexes **2** and **3** show similar features in the Nyquist plots. The hemicircle apparent in the high-frequency region is attributed to the charge-transfer process of molecules at the FTO/electrolyte interface. The straight line in the intermediate frequency region arises from hole percolation through the SAM coupled to semi-infinite length diffusion of counterions present in the mesoporous film. The almost vertical line in the low-frequency region confirms the capacitive behavior of the TiO_2/complex/electrolyte interface, as described by the equivalent circuit in Figure 1. Note that the transport impedance of **3** is much higher than that of **2**. Curve fitting gives the characteristic time constant τ_d, which is related to the hole diffusion coefficient by the equation

$$D_+ = L^2/\tau_d \qquad (3)$$

where L is the film thickness. The values determined are 2.6×10^{-8} and 1.4×10^{-9} cm^2/s for **2** and **3**, respectively. These are somewhat higher than the diffusion coefficients determined by the CV measurements, in keeping with expectations.[15] Given that the molecular structures of the two complexes are closely related, the dramatic difference in the surface hole conduction behaviors of **2** and **3** must be attributed to the involvement of vicinal sulfur atoms from the thiocyanate groups in the charge hopping process.

This contention is further supported by the observation that exposure of the mesoscopic oxide film covered with a monolayer of **1** or **2** to a Hg^{2+} containing solution suppresses the cross surface hole transfer. As shown in Figure 9, complex **2** lost its capability for charge conduction after dipping the film in 25 mM $HgCl_2$/acetonitrile solution for few seconds. Concomitantly, the maximum of the absorption band shifts from 520 to 470

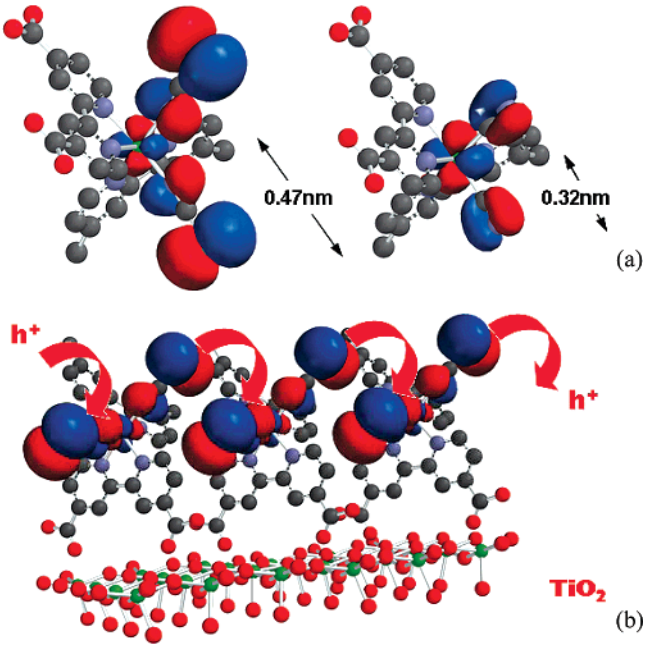

Figure 7. (a) HOMO of complex **2** and **3**. (b) Schematic model showing the configuration of complex **2** on the (101) surface of anatase TiO_2. Individual structures were optimized using Spartan ab initio Software. The location of complex **2** on the TiO_2 surface followed the arguments in ref 23.

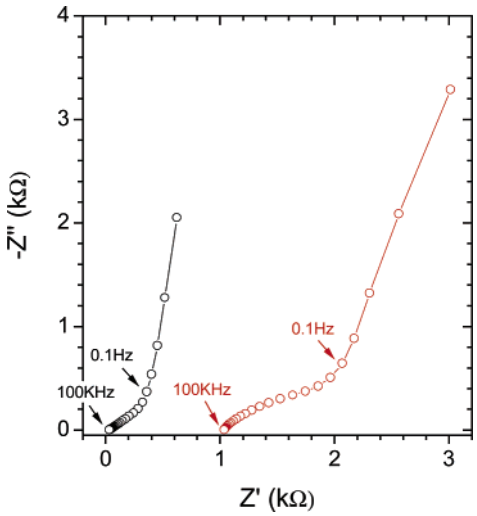

Figure 8. Nyquist plots of mesoscopic TiO_2 electrodes covered with an SAM of complex **2** (black) or **3** (red) at 0.25 and 0.45 V (vs Fc+/Fc), respectively. The electrolyte is 0.1 M $TBAPF_6$/acetonitrile. For clarity of presentation, the real part of the red curve is positively shifted by 1 KΩ.

nm, and the color of the dyed film changes from red to orange,[24] as indicated by the UV/vis spectra shown as an inset of Figure 9. The strong interaction between the −NCS groups complex and Hg^{2+} is also well demonstrated by IR measurements. The N═C═S stretching mode shown in Figure 6 is strongly diminished after dipping in Hg^{2+} containing solution while there is almost no change of the other vibration modes. This confirms that the sulfur *p*-orbitals undergo strong binding with mercuric ions,[25] preventing their participation in the intermolecular

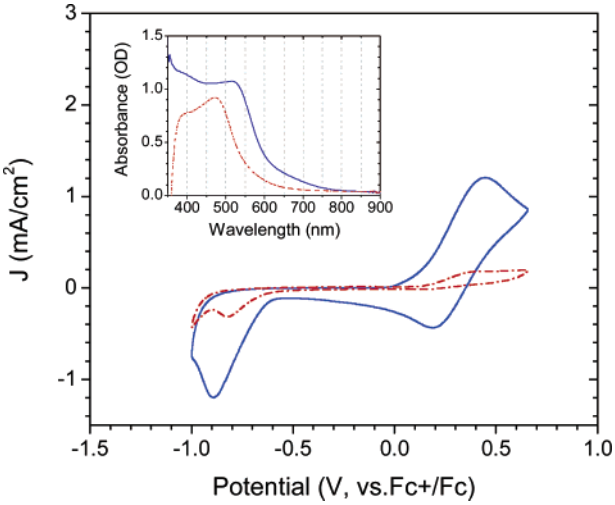

Figure 9. CV of complex **2** adsorbed on mesoscopic TiO_2 before (dark blue) and after dipping in 25 mM $HgCl_2$/acetonitrile solution for a few seconds (dashed orange). The electrolyte is 0.1 M EMITFSI/acetonitrile. The scan rate is 0.1 V/s. The inset shows the UV/vis spectra of complex **2** adsorbed on mesoscopic TiO_2 before (dark blue) and after dipping in Hg^{2+} containing solution (dashed orange).

Table 1. Oxidation Potentials and D_+ of Charge Percolation in a Monolayer of Complex Adsorbed on Mesoscopic TiO_2 Films[a]

complex	E_{OX}, V (vs Fc)	$D_{h+,AN}$,[b] 10^{-9} cm²/s	$D_{h+,EMITFSI}$,[c] 10^{-9} cm²/s
1	0.30	4.1 (7.3[e])	1.5
2	0.31	11.4 (26.0[f])	3.8
3	0.58	1.9 (1.4[f])	0.09
4	0.38		
5	0.87	0.3[d]	
6	0.92	0.02	
7	0.38	0.5	

[a] The above data were obtained from CV measurements. [b] Using 0.1 M EMITFSI/acetonitrile as the electrolyte. [c] Using pure EMITFSI as the electrolyte. [d] Using 0.1 M $TBAPF_6$/acetonitrile as the electrolyte. [e] Obtained from chronocoulometric measurement using 0.1 M EMITFSI/acetonitrile as the electrolyte (see Figure S1). [f] Obtained from impedance measurements using 0.1 M $TBAPF_6$/acetonitrile as the electrolyte.

electron exchange and blocking in this fashion the cross surface hole transfer process.[26]

Table 1 displays the oxidation potentials and the charge percolation rates of series of Ru-complexes anchored on mesoscopic TiO_2 films. Note that in the adsorbed state the oxidation potentials of these compounds are higher than in solution.[8a,27] This arises from the complexation of the carboxylate groups by surface Ti^{4+} ions. Among the studied complexes, **2** possesses the highest hole diffusion coefficient the value being between 1.1×10^{-8} cm²/s and 2.6×10^{-8} cm²/s, which is comparable to that of the triarylamine.[4a] In comparison, the diffusion coefficient for holes in a monolayer of **3** is more than 40 times smaller than that of **2**, when EMITFSI is used as the electrolyte, and that of the hydrophobic molecule **6** is more than 200 times smaller than that of **1** using 0.1 M EMITFSI/acetonitrile as the electrolyte. The observation that the charge percolation rate of complex **2** is higher than that of **1** is likely

(23) Shklover, V.; Ovchinnikov, Y. E.; Braginsky, L. S.; Zakeeruddin, S. M.; Grätzel, M. *Chem. Mater.* **1998**, *10*, 2533−2541.
(24) (a) Coronado, E.; Galan-Mascaros, J. R.; Marti-Gastaldo, C.; Palomares, E.; Durrant, J. R.; Vilar, R.; Grätzel, M.; Nazeeruddin, Md. K. *J. Am. Chem. Soc.* **2005**, *127*, 12351−12356. (b) Nazeeruddin, Md. K.; Censo, D. Di; Humphry-Baker, R.; Grätzel. M. *Adv. Funct. Mater.* **2006**, *16*, 189−194.
(25) Chae, M. Y.; Czarnik, A. W. *J. Am. Chem. Soc.* **1992**, *114*, 9704−9705.
(26) One of the referees suggested that coordination of Hg^{2+} increases the size of the ruthenium compound and decreases the accessibility of the surface bound complex to charge compensation ions, which could lower the rate of cross-surface charge percolation.
(27) Wang, P.; Zakeeruddin, S. M.; Comte, P.; Charvet, R.; Humphry-Baker, R.; Grätzel, M. *J. Phys. Chem. B* **2003**, *107*, 14336−14341.

to result from a higher surface concentration[28] and more effective screening of the positive charge by counterions from the electrolyte. The long hydrophobic alkyl chain of complex **1** blocks the access of anions to the oxide surface rendering charge compensation less facile than in the case of **2**.[4]

Importantly, the orientation of the NCS groups has also a pronounced effect on the cross surface hole transport process. For example, the well-known N3 sensitizer *cis*-$RuL_2(SCN)_2$ (**4**) adsorbs on the surface via the two carboxylic groups, which are in the *trans* position to the −NCS ligands.[21] As a result, the spatial separation between the −NCS ligands of neighboring molecules in the adsorbed state is significantly larger compared to complex **2**. Results from spectroelectrochemical measurements of complex **4** adsorbed on a mesoscopic TiO_2 film are shown in Figure 4b. Upon positive polarization, a new band appears at around 720 nm, which has been assigned to an LMCT transition of the Ru(III) complex.[12] A set of isosbestic points was observed upon scanning the potential from −0.4 to 0.5 V indicating that the oxidation is again a simple one-electron process. However, when the anodic limit was extended to 0.75 V, as in the cyclic voltammogram reported in Figure S2a, no cathodic wave appeared on the reverse scan in the acetonitrile-based electrolyte indicating that the oxidation was irreversible. It became partially reversible in the EMITFSI ionic liquid. Spectral data suggest that the molecule appears to degrade if the dyed film is kept at high potential for an extended time. The Ru(II/III) potential is 80 mV higher for complex **4** as compared to complex **1** favoring a destructive internal redox reaction, e.g., ligand oxidation, to occur. From the decrease of the absorbance of an MLCT transition, it can be inferred that only a few percent of complex **4** adsorbed on the surface of the mesoscopic TiO_2 film are oxidized upon positive polarization. Because of the unfavorable orientation of the NCS ligands, charge percolation is very inefficient and only the complexes adsorbed in the region of the mesoscopic TiO_2 film that is adjacent to the FTO are implied in the redox reaction. In addition, the irreversible oxidation of the complex in proximity to the substrate at high potential would also impede the charge percolation. In comparison, the conversion of complex **1** is much larger under the same conditions.

Similarly the low anodic current observed with $RuL'''(SCN)_2$ (L‴ = 4,4′-Bis[*p*-carboxylic acid]-2,2′:6′,2″:6″,2‴-quaterpyridine) (**7**) is assigned to unfavorable orientation of −NCS on the surface of the metal oxide similar to **4** due to trans −NCS ligands, which prevents effective HOMO overlap and reducing the rate of hole hopping between adjacent sensitizer molecules as shown in Figure S2b.

Finally we found that the complex $[Ru^{II}(dmbpy)_2(4,4'\text{-dcbpy})]Cl_2$ (**5**) shows very sluggish charge percolation. Cyclic voltammetry measurements performed with the solution of **5** in acetonitrile are shown in Figure S3. From the scan rate dependence of the peak current the hole diffusion coefficient is derived to be only 3.0×10^{-10} cm^2/s. Under similar conditions the analogous Os complex $[Os^{II}(bpy)_2(4,4'\text{-dcbpy})](PF_6)_2$ gave a 5 times higher value of the diffusion coefficient.[7a] This difference is presumably attributed to the larger spatial extension of the *5d*-orbitals of osmium compared to those of ruthenium producing stronger electronic coupling between neighboring Os complexes, thereby enhancing the hole migration.

Conclusions

Ambipolar charge transport confined to a self-assembled monolayer of a heteroleptic ruthenium complex anchored on the surface of mesoscopic oxides was observed for the first time. The bipyridyl ligands of the Ru-complex transport electrons, while the NCS groups plays a pivotal role in mediating surface-confined hole percolation. Cyclic voltammetric, spectroelectrochemical, and impedance measurements were applied to determine the percolation threshold and rate for cross surface hole transfer. By testing a series of Ru-complexes, the heteroleptic complexes **1** and **2** emerged by far as the most efficient surface hole conductors. The high charge percolation rates could arise from a relatively low energy barrier for electron exchange and an enhanced electronic coupling between vicinal NCS-groups. The electronic interaction is enhanced by the specific molecular constellation imposed by the geometry and packing constraints, which complexes **1** and **2** are subjected to in the adsorbed state. Our findings shed new light on the factors that control these intriguing cross surface charge percolation processes in mesoscopic systems, for which numerous applications ranging from photovoltaic cells to sensors and switchable molecular electronics can be foreseen.

Acknowledgment. We acknowledge financial support of this work by the U.S. Airforce European Office for Research and Development and the Swiss National Science Foundation. We thank Mr. P. Comte and R. Charvet for preparing the mesoscopic oxide films.

Supporting Information Available: Cottrell plot of complex **1**, cyclic voltammograms of complex **4**, **5**, and **7** in different electrolytes and scan rates, and complete ref 19b. This material is available free of charge via the Internet at http://pubs.acs.org.

JA058616H

(28) UV/vis absorption spectroscopic measurements indicate the uptaking of complex **3** on TiO_2 film is comparable to complex **2**. Whereas the uptake of complex **2** is 5.7% higher than that of **1**.